



Research Article

# A Green approach for the synthesis of iron oxide nanoparticles by using roots of *A. racemosus* and its degradation of dye methyl orange.

P.P.N.Vijay Kumar<sup>a</sup>, S.V.N.Pammi<sup>b</sup>, U. Shameem<sup>c</sup>

<sup>a</sup>Advanced Analytical laboratory, College of Science and Technology, Andhra University, Visakhapatnam 530003, India.

<sup>b</sup> Department of Materials Science and Engineering, Chungnam National University, Daeduk Science Town, 305-764, Daejeon, Korea.

<sup>c</sup>Department of Zoology, College of Science and Technology, Andhra University, Visakhapatnam 530003, India.

Date Received: 27<sup>th</sup> December 2017; Date accepted: 1<sup>st</sup> January 2017; Date Published: 3<sup>rd</sup> January 2018

## Abstract

Metal oxide nanoparticles have been used in various fields ranging from catalysis and optoelectronic materials to sensors, environmental remediation and biomedicine. The present study reports green synthesized Fe<sub>2</sub>O<sub>3</sub> nanoparticles by using roots of *A. racemosus*. This approach involves ecofriendly and non-toxic method. Powder X-ray diffraction, scanning electron microscope and transmission electron microscope analysis revealed that synthesized Fe<sub>2</sub>O<sub>3</sub> nanoparticles are in spherical shape with an average particle size of 40 nm. The synthesized iron oxide nanoparticles are uti-

lized as green catalyst for the effective degradation of dye methyl orange.

**Key words:** *A. racemosus*, Iron oxide, Green synthesis, methyl orange

## INTRODUCTION

Magnetite nanoparticles have drawn great attention for many important technological and biomedical applications such as magnetic separation, drug delivery, cancer hyperthermia and magnetic resonance imaging (MRI) enhancement, due to their non-toxicity property and high chemical stability. Green approach of nanoparticles using plant extracts and microorganisms (bacteria, fungi, algae, and yeast) play a significant role in iron oxide nanoparticles synthesis from naturally biodegradable matter. Among these, synthesis by plant extracts is advantageous as it reduce the risk of further contamination by decreasing the reaction time and maintaining the cell structure (1). These plant extracts have proven to be non-toxic to living organisms, a reproducible resource and environmental friendly material containing secondary metabolites. These act as both reducing and stabilizing agents when they are used to synthesize metal and metal oxide nanoparticles via greener approach. In addition, plant extracts acting as both reducing agent and capping/stabilizing agent are generating much interest. Hence the green synthesis is proposed to be a suitable alternative candidate to conventional methods as there is an increasing demand on ecofriendly, cost effective and less toxic way of synthesizing nanoparticles (2,3,4). Iron-based nanoparticles have been successfully used in the field of environmental remediation and toxic waste treatment (5,6). Due to their high specific surface area size and high reactivity, iron-based nanoparticles can remove various dyes contaminants including malachite green (5), scarlet 4BS (7) and orange G (8). This is despite dyes being quite difficult to remove from aqueous solutions (9), which are often potentially dangerous to the environment (10). Furthermore, recent studies have proposed that iron-based nanoparticles do have short comings, such as aggregating into chain-like structures, and oxidation by non-target com-

pounds. To address these issues, supporting materials such as bentonite (7), and surface stabilizers such as Tween-20 (11), starch (12), and chitosan (13) have been used to disperse iron-based nanoparticles. In the present study we used roots of *A. racemosus*, it is commonly known as 'Shatavari', means "she who possesses a hundred husbands" (14) belongs to the family Liliaceae. *A. racemosus* contains various phytochemicals like alkaloids, glycosides, saponins and tannins (15) responsible for the synthesis of iron oxide nanoparticles. The synthesized  $\text{Fe}_2\text{O}_3$  have been utilized for catalyzing the decolourization of methyl orange assisted with  $\text{H}_2\text{O}_2$ .

## 2. Materials and methods:

### 2.1 Preparation of extract

*Asparagus racemosus* herbal plants were collected from local area of Andhra University campus, authenticated and deposited in Botany department herbarium (B.D.H), voucher number AU (B.D.H) - 22083 respectively. The roots were separated and repeatedly washed with double distilled water and air dried. The rootstocks are tuberous, bearing numerous fusiform and the Succulent tuberous roots are 30-100 cm long and 1-2 cm thick. The roots were made in to fine powder using domestic blender and aqueous extract was prepared using soxhelt apparatus.

### 2.2 Synthesis of Iron Oxide Nanoparticles:

An aliquot of 10 ml of aqueous root extract was mixed with 100 ml of 1M  $\text{FeCl}_3 \cdot 6\text{H}_2\text{O}$  for reduction of  $\text{FeCl}_3$ . The reaction was carried out under stirring and boiling for 3 hours. Further, the mixture was cooled to room temperature and centrifuged at 10,000 rpm for 10 min. The obtained wet precipitate was washed thrice with ethanol and DDW to eliminate the impurity. The collected Iron oxide NPs were allowed to dry and formed precipitate was ground for further characterization.

### 2.3. Characterization of Iron Oxide Nanoparticles:

The morphological, structural, thermal and chemical composition of nanoparticles were analyzed with SEM -EDX (JEOL JSM-6610-LV- with OXFORD EDS), XRD (PANalytical: XPERT-PRO) and FTIR (Shimadzu FT-IR 21) Prestige equipment. Transmission Electron Microscopic (TEM) analysis

was done by using a TEM, JEM-1200EX, JEOL Ltd., Japan. TGDTA (STA7300- HITACHI). The dye degradation of iron oxide nanoparticles were studied by UV-VIS (Shimadzu UV-VIS 2450) spectral analysis.

### 2.4. Photo catalytic degradation of Methyl Orange by $\text{Fe}_2\text{O}_3$

Photocatalytic degradation of methyl orange (MO) was performed under irradiation of UV light for various time intervals. 1mM of MO was prepared and required concentrations were prepared by dilution from 1mM MO. For the degradation of MO add 100  $\mu\text{L}$   $\text{H}_2\text{O}_2$  mixture, and 100  $\mu\text{L}$  of green synthesized FeONPs were added to verify the catalytic effect of the FeONPs on the decolourization process. The degradation of MO was monitored by measuring the absorbance at regular time intervals using UV-Visible spectrophotometer at  $\lambda$ - 465 nm.

## 3. Result and Discussion:

The structure and chemical composition of  $\text{Fe}_2\text{O}_3$  green synthesized nanoparticles were examined by X-ray diffraction (XRD) pattern. Several well-defined diffraction reflections were seen in the pattern which is well matched with the rhombohedral  $\alpha$ - $\text{Fe}_2\text{O}_3$  structures (Fig.1). The observed results are consistent with the reported literature and well matched with the JCPDS data (JCPDS 89-8104). No other reflections were noticed in the pattern which reveals that the synthesized products are pure  $\alpha$ - $\text{Fe}_2\text{O}_3$ . The average crystalline size of Iron oxide nanoparticles was estimated using the Debye-Scherrer equation and found to be around 40 nm. The morphology of the green synthesized  $\text{Fe}_2\text{O}_3$  nanoparticles were investigated by SEM. As shown in figure 2(a), the morphology of the  $\alpha$ - $\text{Fe}_2\text{O}_3$  has a spherical shape, and the size of the product is rather uniform with diameter of 30-40nm, which was confirmed by the TEM (Fig 3). The elemental composition of nanoparticles is examined by energy dispersive spectroscopy. Figure 2(b) exhibits the typical EDS spectrum of nanoparticles which shows well defined peaks for iron (Fe) and oxygen (O). Except, Fe and O, no other peak related with any other element is found in the spectrum which revealed that the synthesized nanoparticles are made of iron and oxygen.

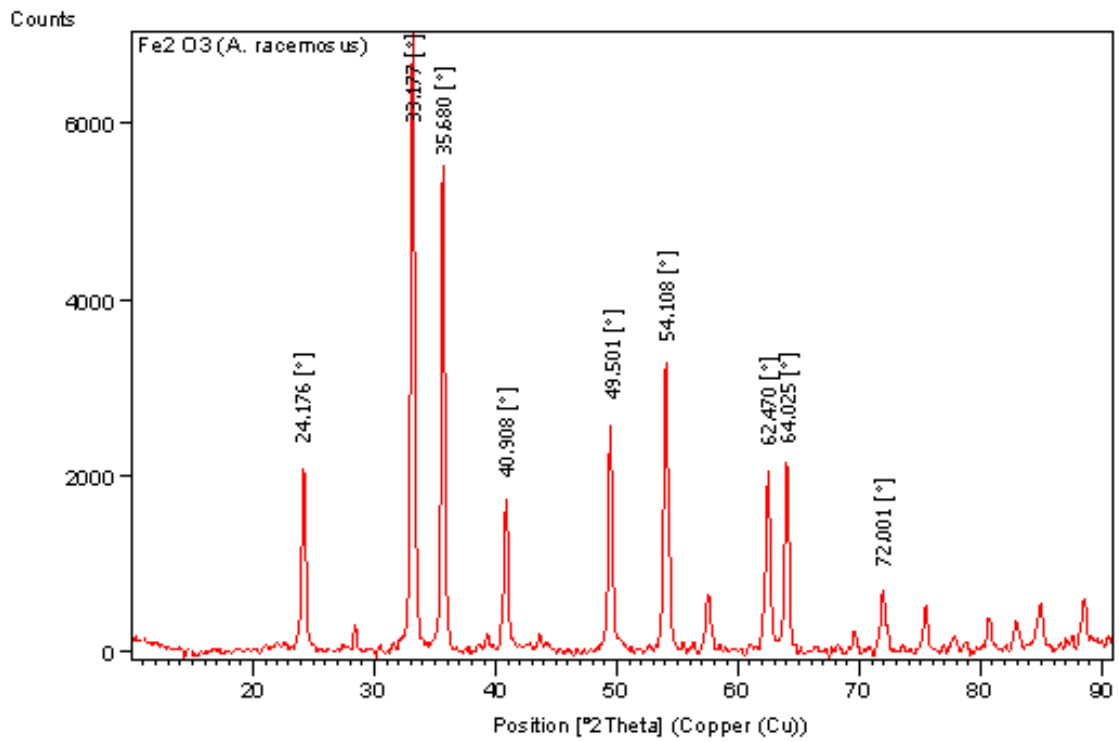


Figure 1: XRD pattern of  $\alpha$ -Fe<sub>2</sub>O<sub>3</sub>

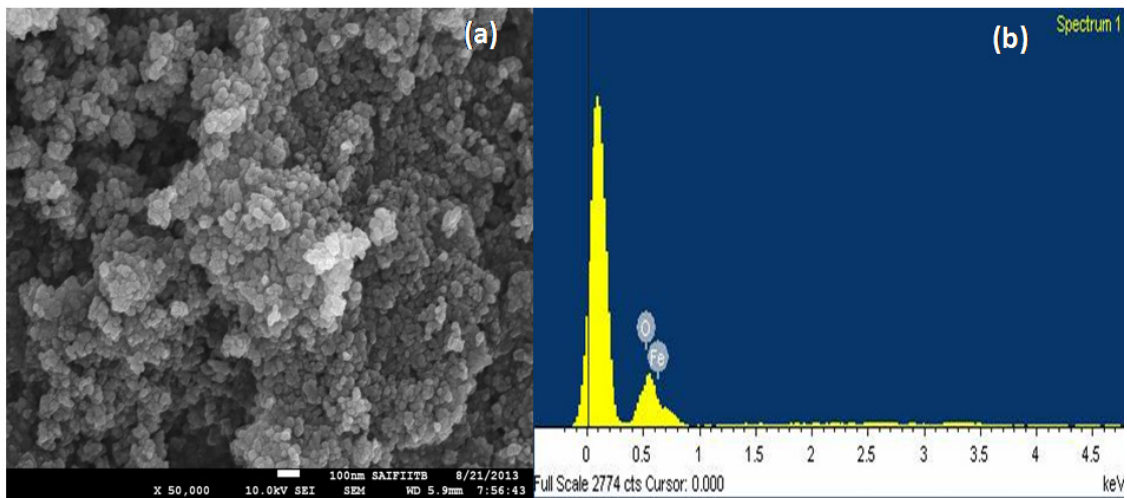


Figure 2: SEM image and EDS spectra of Fe<sub>2</sub>O<sub>3</sub>

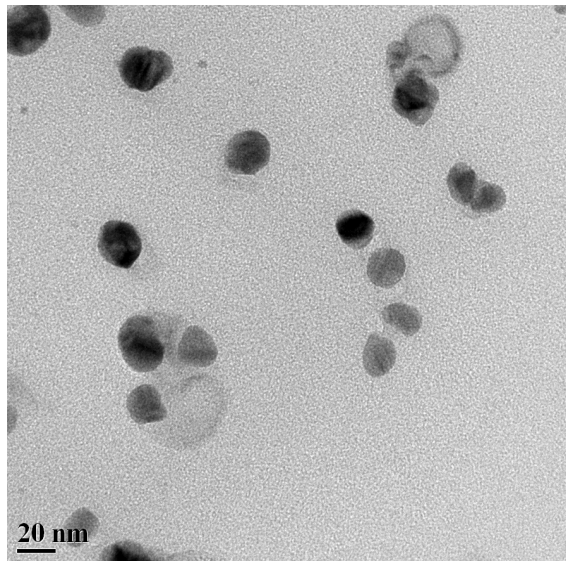


Figure 3: TEM images of Fe<sub>2</sub>O<sub>3</sub>

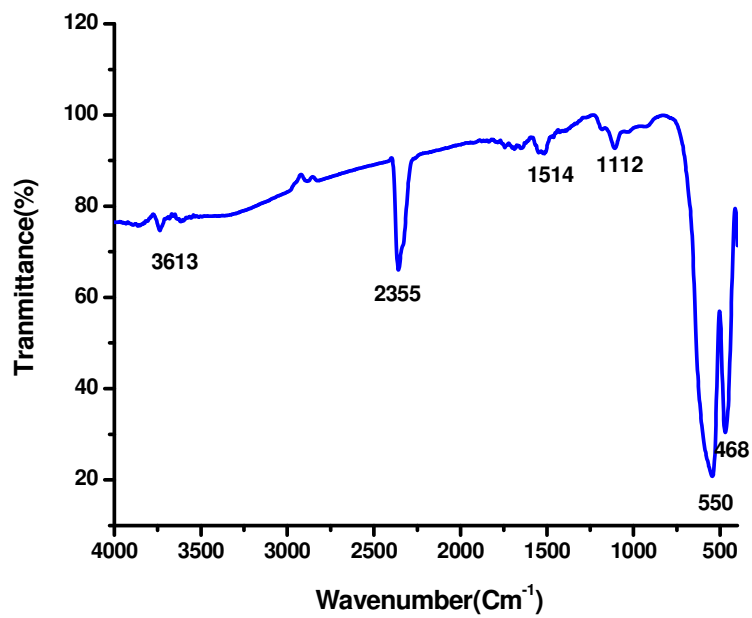


Figure 4. FTIR spectra of Fe<sub>2</sub>O<sub>3</sub>

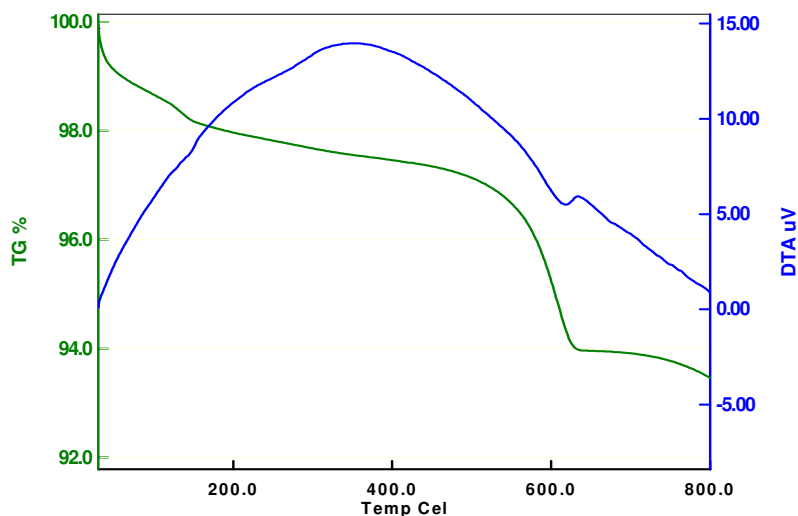


Figure 5. TGDTA spectra of Fe<sub>2</sub>O<sub>3</sub>

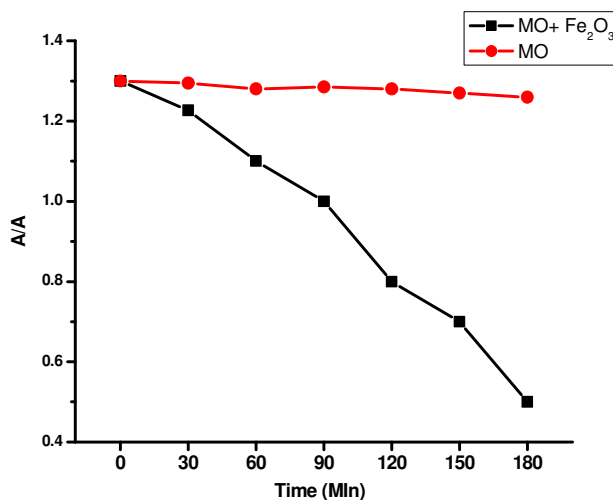


Figure 6. UV spectra of Methyl Orange (MO) degradation by Fe<sub>2</sub>O<sub>3</sub>

FT-IR spectra of the Fe<sub>2</sub>O<sub>3</sub> nanoparticles were recorded to identify the functional groups of the phytoconstituents responsible for the reduction of the metal precursors (Fig.4). The adsorption bands around 460 cm<sup>-1</sup> and 546 cm<sup>-1</sup> corresponded to Fe-O stretches of Fe<sub>2</sub>O<sub>3</sub> (Chen et al., 2011) and other peaks at 1112 cm<sup>-1</sup> corresponds to stretches O-C stretches, 1514 cm<sup>-1</sup> to N=O stretches, 2355 cm<sup>-1</sup> and 3613 cm<sup>-1</sup> stretches to O-H which are proved to be phytoconstituents present in the sample.

TG & DTA curves of Fe<sub>2</sub>O<sub>3</sub> nanoparticles were as shown in Figure 5. The temperature range is 30°C to 800°C. In TG analysis, the total weight loss percentage of the sample is 6.5 %. The initial weight loss 2.3% was observed below 300°C, it corresponds to the liberation of adsorbed moisture on the surface of the sample. At transition range of temperature 300-500°C, the weight loss being 0.5% which is due to the elimination of carbon group compounds. In the final stage, temperature range

from 500-800°C; the weight loss is about 3.7 %. This corresponds to phase transformation from Fe to Fe<sub>2</sub>O<sub>3</sub>. From DTA, one exothermic and one endothermic peak was observed. At 600°C to 700°C both the endothermic and exothermic peaks were observed due to phase transformation. It corresponds to the complete liberation of carbonaceous and other inorganic materials in the sample and it infers that the sample has very extreme purity and very less weight loss.

The absorption spectrum intensity peak at λ- 465 nm of MO was decreased with increasing the irradiation time which confirms that the degradation of MO increases with increase in UV light exposure time (Fig-6). Therefore, it can be concluded that green synthesized Fe<sub>2</sub>O<sub>3</sub> nanoparticles are acting as efficient photo catalyst for the photo catalytic degradation of methyl orange (MO).

#### Conclusion

In this study, Fe<sub>2</sub>O<sub>3</sub> nanoparticles were successfully synthesized using *A. racemosus*, the Fe<sub>2</sub>O<sub>3</sub> nanoparticles possess unique shape and size conformed by SEM, TEM, XRD and FT-IR analyses. All the results demonstrated that the Fe<sub>2</sub>O<sub>3</sub> surface was capped with organic materials that originated from *A. racemosus* extract as a capping or stabilizing agent. The synthesized FeO NPs were effective in catalyzing the degradation of methyl orange dyes with H<sub>2</sub>O<sub>2</sub> as an oxidizer. This could possibly be an efficient route for dye degradation from effluents of industries.

#### Acknowledgements

We are thankful to the DST-PURSE Programme for the financial assistance and Advanced Analytical Laboratory, Andhra University for their support in carrying out in this research work regarding SEM-EDX and XRD, TGDTA, FTIR and UV spectrum analysis. Authors are thankful to SAIF, IIT Bombay for TEM characterization.

#### 4. References

1. Ajitha B, Reddy A K, Reddy P S. Green synthesis and characterization of silver nanoparticles using *Lantana camara* leaf extract, Materials Science and Engineering C, 2015; 49:373-381.
2. Devatha C.P, Arun Kumar Thalla, Shweta Y. Katte. Green synthesis of Iron Nanoparticles using different leaf extracts for treatment of domestic waste water Journal of Cleaner Production, 2016: 139: 1425-1435.
3. Vijay kumar P.P.N, Pammi S.V.N, Pratap Kollu, Satyanarayana K.V.V, Shameem U. Green synthesis and characterization of silver nanoparticles using *Boerhaavia diffusa* plant extract and their anti bacterial activity. Journal of Industrial Crops and Products. 2014;52: 562- 566.
4. Vijay kumar P.P.N, Shameem, U. Pratap Kollu, Kalyani, R.L, Pammi S.V.N. Green synthesis of copper oxide nanoparticles using *Aloe Vera* leaf extract and its antibacterial activity against fish bacterial pathogens.. Bio nano science. DOI 10.1007/s12668-015-0171-z
5. He, Y., Gao, J.F., Feng, F.Q., Liu, C., Peng, Y.Z., Wang, S.Y. The comparative study on the rapid decolorization of azo, anthraquinone and triphenylmethane dyes by zero-valent iron. Chem. Eng. J. 2012;179, 8-18.
6. Lin, Y.M., Chen, Z.L., Megharaj, M., Naidu, R., Degradation of scarlet 4BS in aqueous solution using bimetallic Fe/Ni nanoparticles. J. Colloid Interface Sci. 2012; 381, 30-35.
7. Chen, Z.X., Jin, X.Y., Chen, Z.L., Megharaj, M., Naidu, R., Removal of methylorange from aqueous solution using bentonite-supported nanoscale zero-valent iron. J. Colloid Interface Sci. 2011; 363, 601-607.
8. Bokare, A.D., Chikate, R.C., Rode, C.V., Paknikar, K.M., Iron-nickel bimetallic nanoparticles for reductive degradation of azo dye orange G in aqueous solution. Appl. Catal. B Environ. 2008; 79, 270-278.
9. Gao, G.D., Zhang, A.Y., Zhang, M., Chen, J.L., Zhang, Q.X., Photocatalytic degradation mechanism of malachite green under visible light irradiation over novel biomimetic photocatalyst HMS-FePcs. Chin. J. Catal. 2008.; 29, 426-430.
10. Shahwan, T., AbuSirriah, S., Nairat, M., Boyac, E., Eroglu, A.E., Scott, T.B., Hallam, K. R. Green synthesis of iron nanoparticles and their application as a Fenton-like catalyst for the degradation of aqueous cationic and anionic dyes. Chem.Eng. J. 2011; 172, 258-266.
11. Kanel, S.R., Nepal, D., Manning, B., Choi, H., Transport of surface-modified nanoparticle in porous media and application to arsenic (III) remediation. J. Nanopart. Res. 2007; 9, 725-735.

12. Alidokht, L., Khataee, A.R., Reyhanitabar, A., Oustan, S., 2011. Reductive removal of Cr(VI) by starch-stabilized Fe<sup>0</sup>nanoparticles in aqueous solution. *Desalination* 270, 105–110.
13. Geng, B., Jin, Z.H., Li, T.L., Qi, X.H. Kinetics of hexavalent chromium removal from water by chitosan–Fe<sup>0</sup>nanoparticles. *Chemosphere*, 2009; 75, 825–830.
14. Barry, A.L., Fuchs, P.C. and Brown, S. D. (1997). Macrolide resistance among *Streptococcus pneumoniae* and *Streptococcus pyogenes* isolates from out-patients in the USA. *Journal of Anti- microbial Chemotherapy*, 40: pp 139–140.
15. Vijay Kumar, P. P. N, Pammi, S.V.N, Gowri Devi K., Shameem U. Phytochemical screening of three herbal plants and their antimicrobial activity against various fish bacterial pathogens *International Journal of Pharmacy*. Photon 105 (2014) 431-435.